Soft Matter

View Online / Journal Homepage
Dynamic Article Links

Cite this: DOI: 10.1039/c1sm06736b

www.rsc.org/softmatter

COMMUNICATION

Harnessing snap-through instability in soft dielectrics to achieve giant voltage-triggered deformation

Christoph Keplinger,[ab] Tiefeng Li,[bc] Richard Baumgartner,[a] Zhigang Suo*[b] and Siegfried Bauer*[a]

Received 13th September 2011, Accepted 7th October 2011
DOI: 10.1039/c1sm06736b

A soft dielectric membrane is prone to snap-through instability. We present theory and experiment to show that the instability can be harnessed to achieve giant voltage-triggered deformation. We mount a membrane on a chamber of a suitable volume, pressurize the membrane into a state near the verge of the instability, and apply a voltage to trigger the snap without causing electrical breakdown. For an acrylic membrane we demonstrate voltage-triggered expansion of area by 1692%, far beyond the largest value reported in the literature. The large expansion can even be retained after the voltage is switched off.

When subjected to a voltage, a soft dielectric membrane reduces thickness and expands area. This robust electromechanical coupling has led to diverse designs of soft transducers, with attributes such as large strain, high energy density, light weight and low noise.[1–5] Emerging applications include soft robots, adaptive optics, balloon catheters, Braille displays, and energy harvesting.[6–8] While a soft membrane can be readily stretched to many times its initial area by mechanical forces, achieving such a large deformation by voltage has been difficult. A maximum voltage-induced area expansion of 380% was reported,[1] much lower than that achievable with mechanical forces. As the voltage increases and the membrane thins down, the electric field amplifies and may result in a type of instability, known as pull-in or snap-through instability.[9–11] The instability often leads to electrical breakdown.[12] Similar instability has been used to manipulate the permeability of cell membranes,[13,14] currently exploited as electroporation in gene transfer, drug delivery, animal cloning and other bioengineering applications.[15]

A recent theory indicates that the snap-through instability can be made safe to achieve giant voltage-triggered deformation with specifically designed soft dielectrics.[16] Here we take a different approach. We ask whether large deformation comparable to that achievable with mechanical forces can be triggered electrically using off-the-shelf materials. We introduce the following principle of operation that enables large voltage-triggered deformation for any soft dielectric: *place a soft dielectric membrane in a state near the verge of the instability, trigger the snap with a voltage, and avert electrical breakdown by a suitable loading path*. Using a combination of theory and experiment, with a commercially available acrylic elastomer (3M™VHB™4910), we demonstrate voltage-triggered expansion of area by 1692%, well beyond the largest value of 380% reported in the literature.[1] It must be stressed that the principle can also be used to guide the design of other transducer configurations and other dielectric elastomer membranes. Furthermore, we show that the large expansion can be retained after the voltage is turned off. The membrane can be designed to have two stable states of equilibrium. One state can be switched to the other with voltage, but the voltage is not needed to maintain either state. Bistable dielectric elastomer actuator systems are currently explored as prime candidates for binary robotic systems,[17] which make use of multiple bistable actuator elements to achieve the accuracy necessary for practical applications.[18] In that context our results may provide new options in designing soft transducers, inspiring a cornucopia of applications.

We demonstrate the physical principle that allows for voltage-triggered safe snap-through instability and bistability in soft membranes with a commonly used actuator design, Fig. 1.[19] A soft dielectric membrane is sandwiched between carbon-grease electrodes, and is mounted on a chamber. When air is pumped into the chamber through a valve, the membrane becomes a balloon of an

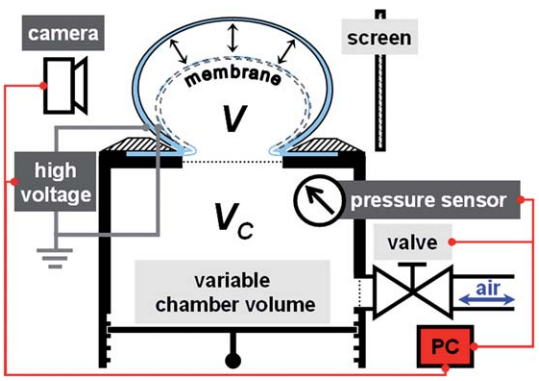

Fig. 1 A soft dielectric membrane, mounted on a chamber, is pressured into a balloon. Afterwards, the valve is closed, and voltage is applied to cause the balloon to expand further. The volume of the balloon is tracked with a video camera, while the pressure in the chamber is recorded with a pressure sensor.

[a]*Soft Matter Physics, Johannes Kepler University, Altenbergerstrasse 69, A-4040 Linz, Austria. E-mail: sbauer@jku.at*
[b]*School of Engineering and Applied Sciences, Harvard University, Cambridge, Massachusetts, 02138, USA. E-mail: suo@seas.harvard.edu*
[c]*Institute of Applied Mechanics, Zhejiang University, 38 Zheda Road, Hangzhou, Zhejiang, 310027, China*

axisymmetric shape. The valve is then closed, fixing the amount of air enclosed by the chamber and balloon. A voltage is subsequently applied between the two carbon-grease electrodes, causing the balloon to expand further. The volume of the balloon is tracked with a video camera, while the pressure in the chamber is recorded with a pressure sensor.

Several aspects of this experimental setup enable the voltage to trigger giant deformation, Fig. 2. First, in the absence of voltage, the pressure–volume relation of the membrane is an *N*-shaped curve—rising, falling, and rising again. If the pressure is controlled to ramp up, the membrane will undergo the purely mechanical snap-through instability, a phenomenon well studied in the literature on rubber balloons.[20]

Second, the chamber can be pressurized to inflate the membrane into a state near the verge of the snap-through instability. Thereby mechanical energy is stored in the system and the energy barrier to electrically trigger the instability is reduced to a convenient level, depending on how far away the initial state is prepared from the onset of instability. As we will show, the voltage shifts the *N*-shaped curve to lower levels of pressure. When the peak of the curve is below the pressure in the chamber, the balloon snaps from a small volume to a large volume; see the inset of Fig. 2. The expansion is accompanied by a drastic thinning of the membrane, often leading to electrical breakdown.

Third, to avert electrical breakdown, we require the pressure to decrease as the balloon snaps to a large volume. This loading path is realized by choosing a chamber of a suitable volume, an essential feature that differentiates our experimental setup from existing approaches. When the volume of the chamber is large, the expansion of the balloon affects the pressure negligibly, and the loading path is the horizontal dashed line, causing electrical breakdown. When the volume of the chamber is small, however, the expansion of the balloon causes the pressure to drop, and the loading path is the tilted dashed line in Fig. 2, averting electrical breakdown.

The loading path can be predicted by assuming that air is an ideal gas:

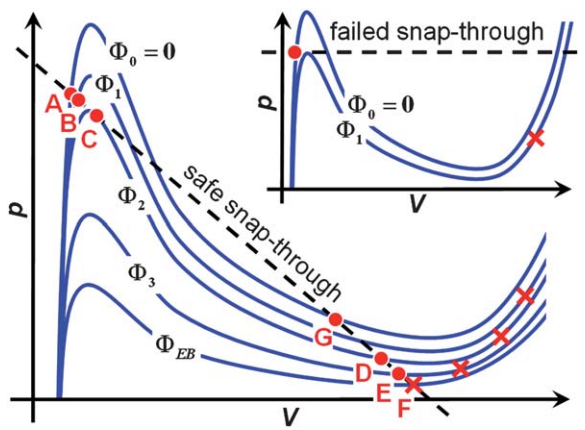

Fig. 2 Solid curves are the pressure–volume relations of a membrane subject to constant values of voltage, with conditions of electrical breakdown marked by crosses. When a large chamber is used, the pressure remains constant when the voltage triggers the snap-through instability, leading to electrical breakdown (inset). When a medium-sized chamber is used, the pressure drops as the voltage triggers the snap-through instability, averting electrical breakdown.

$$NkT = (p + p_{\mathrm{atm}})(V + V_{\mathrm{C}}), \tag{1}$$

where p is the excess pressure of the air in the chamber relative to the atmospheric pressure p_{atm}, V_{C} is the volume of the chamber, V is the volume of the balloon, N is the number of air molecules, and kT is the temperature in the unit of energy. The amount of air enclosed by the chamber and balloon is fixed after the valve is closed. The deformation is assumed to be isothermal. Eqn (1) is sketched in Fig. 2 as the dashed curve.

Also sketched in Fig. 2 are pressure–volume curves of the membrane subject to several constant levels of voltage. In the absence of voltage, $\Phi_0 = 0$, the chamber is pressurized to inflate the membrane into state A, which is slightly below the peak pressure. This state is the intersection of the pressure–volume curve of the air and that of the membrane in the absence of voltage. When voltage Φ_1 is applied, the balloon expands slightly to a new state of equilibrium B, which is the intersection of the pressure–volume curve of the air and that of the membrane subject to voltage Φ_1. At a larger voltage Φ_2, the pressure–volume curve of the air becomes tangent to that of the membrane and the balloon snaps from state C to state D. By choosing a chamber of a suitable volume, the state D can be made to avert electrical breakdown. Additional increments of voltage result in a small further expansion to state E, and eventually cause electrical breakdown at Φ_{EB} in state F. When the voltage is switched off in state D, the balloon retracts to state G. Both A and G are states of equilibrium. That is, in the absence of voltage, the membrane mounted on an air-filled chamber is a structure of two stable states of equilibrium.

The membrane undergoes inhomogeneous deformation. At the edge of the membrane, the latitudinal stretch is fixed by the rim, while the longitudinal stretch increases as the balloon expands. The apex of the balloon, however, is in a state of equal-biaxial stretch. The inhomogeneous deformation can be analyzed by solving a nonlinear boundary-value problem. Following much of the existing literature, we adopt the model of ideal dielectric elastomers,[10] so that the Helmholtz free energy is a sum of the elastic energy due to the stretching of the elastomer, and the electrostatic energy due to the polarization of the elastomer. To model the snap-through instability, we need to account for stiffening of the elastomer at large deformation. The density of the Helmholtz free energy is taken to be of the form

$$W = -\frac{\mu J_{\mathrm{lim}}}{2}\log\left(1 - \frac{\lambda_1^2 + \lambda_2^2 + \lambda_3^2 - 3}{J_{\mathrm{lim}}}\right) + \frac{D^2}{2\varepsilon}, \tag{2}$$

where λ_1, λ_2 and λ_3 are the stretches, D is the electric displacement, and ε is the permittivity. The first part in (2) represents the elastic energy by the Gent model,[21] with μ being the small-stress shear modulus, and J_{lim} a constant that accounts for the stiffening at large deformation. The elastomer is taken to be incompressible, $\lambda_1\lambda_2\lambda_3 = 1$.

The free energy of the membrane is an integral over the area of the membrane, $\int W \mathrm{d}A$. When the volume of the balloon varies by δV, the excess pressure does work $p\delta V$. When the amount of charge on either electrode varies by δQ, the voltage does work $\Phi\delta Q$. A state of equilibrium is attained when the variation of the free energy of the membrane equals the combined work done by the pressure and the voltage:

$$\delta\int W \mathrm{d}A = p\delta V + \Phi\delta Q. \tag{3}$$

This condition of equilibrium, together with the kinematics of the experimental setup, leads to a set of differential equations,[22,23] which we solve numerically. Numerical results in ref. 22 were restricted to spherical shapes, and those in ref. 23 did not include the snap-through instability. To effectively capture the snap-through instability, here we prescribe stretch at the apex, solve the differential equations and determine the pressure by the shooting method.

The membrane used in the experiments is of radius $A = 2.25$ cm and the initial thickness $H = 0.1$ cm. To minimize the effect of viscoelasticity of the acrylic elastomer, the rate of inflation in a preliminary experiment to extract the mechanical material parameters is chosen so that the time from the initial shape to a state near material rupture matches the time scale of the subsequent experiments. Fitting of the pressure–volume data (not shown) gives $\mu = 45$ kPa and $J_{\lim} = 270$. The atmospheric pressure in the measurements is 101.325 kPa. The relative permittivity of the elastomer is 4.7.[24] At the apex, the balloon is in a state of equal-biaxial stretch, $\lambda_1 = \lambda_2 = \lambda$, and the electric field is maximized, $E = \Phi\lambda^2/H$. The electrical breakdown field varies with the stretch ratios, and the experimental data available for VHB 4910 have been fitted to $E_{EB} = 30.6\lambda^{1.13}$ MV m^{-1}.[25]

Fig. 3 plots the calculated relation between the voltage and the volume of the balloon for membranes mounted on chambers of several volumes. The conditions for electrical breakdown are marked as crosses. Prior to applying the voltage, the pressure is the same in all the chambers, inflating the balloons to the same small volume. For $V_C = 350$ cm^3, the amount of air in the chamber is so small that the voltage cannot cause the balloon to undergo the snap-through instability prior to electrical breakdown. For $V_C = 10\,000$ cm^3, the amount of air in the chamber is sufficient for the voltage to cause the balloon to snap from a small volume to a large volume, and the balloon of the large volume averts electrical breakdown; after the voltage is switched off, the balloon snaps back and recovers the initial state. For $V_C = 20\,000$ cm^3, the amount of air in the chamber is so large that, even in the absence of the voltage, the balloon can be in two stable states of equilibrium, one with a small volume and the other with a large volume; an application of the voltage triggers the balloon to snap, without causing electrical breakdown; after the voltage is switched off, the balloon equilibrates in the stable state of large volume (indicated with a red dot in Fig. 3(c)). For $V_C = 300\,000$ cm^3, the situation is similar to the previous case, except that the snap-through expansion results in electrical breakdown. Voltage-expansion curves of similar trends have been predicted for spherical balloons.[22]

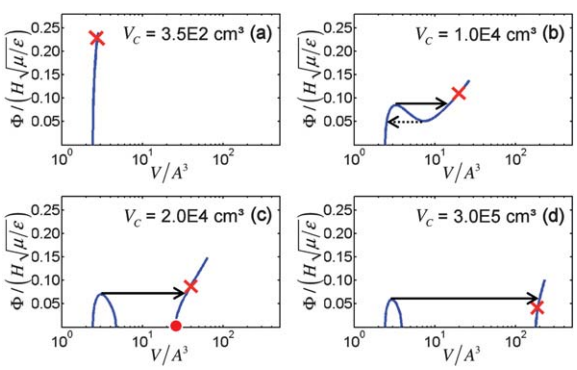

Fig. 3 Voltage plotted as a function of the volume of balloons pressurized by air in chambers with different volumes, the conditions of electrical breakdown are marked by crosses. The horizontal arrows indicate snap-through instabilities.

Fig. 4 summarizes our experimental findings for membranes mounted on chambers of three volumes: 350 cm^3, 20 000 cm^3 and 300 000 cm^3. In every case, air is pumped into the chamber up to a pressure of 19 mbar, which inflates the membrane into a balloon with a volume of 12 cm^3. Thereafter, the amount of air is kept constant by closing the valve, followed by applying a voltage, ramping up to 5.5 kV in 458 s, and then ramping down by the same rate. For $V_C = 350$ cm^3, the voltage does not significantly affect the pressure and volume. For $V_C = 20\,000$ cm^3, the pressure and volume vary slightly when the voltage is below 4 kV; however, when the voltage exceeds this value a snap-through expansion is triggered, indicated by the drop in pressure and the increase in volume to 270 cm^3. When the voltage is ramped down to zero, the initial conditions are not restored, as predicted by the calculation. For $V_C = 300\,000$ cm^3, the instability leads to failure by electrical breakdown. The shapes of the balloon observed in the experiment may be compared with those calculated from the model.

In the calculated shapes, the color codes the latitudinal stretch and reveals inhomogeneous deformation of the balloon. From D to E the color coding at the apex gives a voltage-triggered stretch from 2.24 to 10.1, corresponding to an expansion of area by 1933%. We have also measured experimentally the stretch at the apex by using three tracer particles. Photos are taken at states D and E. An average stretch of 4.23 is measured between the tracer particles, giving an area expansion of 1692% for the experiment shown in Fig. 4(b), in reasonable agreement with the prediction from the model. From ten distinct trials with the experimental conditions specified for Fig. 4(b), we conclude that the presented area expansion value is very robust and a representative value. Due to impreciseness in preparing identical experimental conditions the presented value for area expansion is subject to variations, which we have conservatively determined to be (1692 ± 100)%. We have not intended to optimize experimental conditions to achieve even higher voltage-triggered strains, but our experiment shows that area expansions well beyond the currently reported maximum of 380% are achievable with off-the-shelf materials.

We have also attempted to study the hysteretic behavior in Fig. 3 (b) predicted by the model by using a membrane mounted on a chamber of volume 10 000 cm^3. The experimentally observed behavior, however, is similar to that of Fig. 3(c). The discrepancy is believed to be due to viscoelastic relaxation, which is not accounted for in the present calculation.

In summary, a combination of theory and experiment shows that the snap-through instability can be harnessed to achieve giant voltage-triggered deformation, far beyond the largest values reported in literature. While demonstrated for a specific experimental setup, the principle of operation may inspire a cornucopia of designs and applications as it enables the most conspicuous feature of this technology to be realized: giant deformation triggered by voltage. The particular experimental setup is also suitable for miniaturization.[26] Furthermore, a balloon mounted on a chamber of a suitable volume is a structure of two stable states of equilibrium. One state can be switched to the other by voltage, but voltage is not needed to maintain either state. This bistable behavior is significant to haptic feedback and refreshable Braille displays, and may offer advantages over existing designs.[27,28]

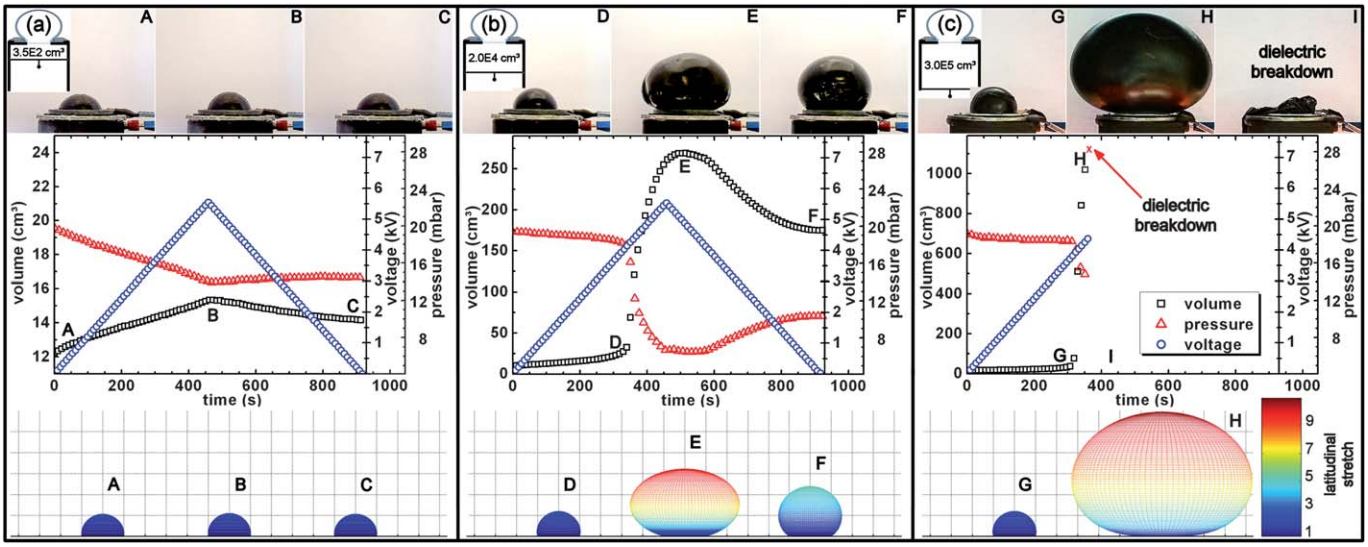

Fig. 4 Membranes are mounted on chambers of different volumes: (a) 350 cm³, (b) 20 000 cm³, and (c) 300 000 cm³. They are pressurized to the same conditions: $p = 19$ mbar and $V = 12$ cm³. Subsequently, the valve is closed, and the amount of air in each chamber remains fixed. In case (a) and (b), the membranes are then subject to a voltage with a triangular pattern. In case (c), the membrane suffers electrical breakdown as the voltage ramps up. The shapes of the membranes at moments A–I are shown by the images taken by the video camera, and by those calculated from the model. The color codes the latitudinal stretch.

This work was partially supported in Linz by the FWF (P20971000N20), and in Harvard by ARO (W911NF-09-1-0476), DARPA (W911NF-10-1-0113), and MRSEC.

References

1 P. Brochu and Q. B. Pei, *Macromol. Rapid Commun.*, 2010, **31**, 10.
2 M. Wissler and E. Mazza, *Sens. Actuators, A*, 2005, **120**, 184.
3 R. Shankar, T. K. Ghosh and R. J. Spontak, *Adv. Mater.*, 2007, **19**, 2218.
4 G. Kovacs, L. During, S. Michel and G. Terrasi, *Sens. Actuators, A*, 2009, **155**, 299–307.
5 R. Pelrine, R. Kornbluh, Q. B. Pei and J. Joseph, *Science*, 2000, **287**, 836.
6 *Dielectric Elastomers as Electromechanical Transducers*, ed. F. Carpi, D. De Rossi, R. Kornbluh, R. Pelrine and P. Sommer-Larsen, Elsevier, 2008.
7 F. Carpi, S. Bauer and D. De Rossi, *Science*, 2010, **330**, 1759.
8 T. G. McKay, B. M. O'Brien, E. P. Calius and I. Anderson, *Appl. Phys. Lett.*, 2011, **98**, 142903.
9 J. S. Plante and S. Dubowski, *Int. J. Solids Struct.*, 2006, **43**, 7727.
10 X. H. Zhao, W. Hong and Z. G. Suo, *Phys. Rev. B: Condens. Matter Mater. Phys.*, 2007, **76**, 134113.
11 C. Keplinger, M. Kaltenbrunner, N. Arnold and S. Bauer, *Proc. Natl. Acad. Sci. U. S. A.*, 2010, **107**, 4505.
12 K. H. Stark and C. G. Garton, *Nature*, 1955, **176**, 1225.
13 H. G. L. Coster and U. Zimmermann, *J. Membr. Biol.*, 1975, **22**, 73.
14 S. Sun, J. T. Y. Wong and T.-Y. Zhang, *Soft Matter*, 2011, **7**, 147.
15 J. C. Weaver and Yu. A. Chizmadzhev, *Bioelectrochem. Bioenerg.*, 1996, **41**, 135.
16 X. Zhao and Z. Suo, *Phys. Rev. Lett.*, 2010, **104**, 178302.
17 P. Chouinard and J. S. Plante, *IEEE/ASME Trans. Mechatron.*, 2011, DOI: 10.1109/TMECH.2011.2135862.
18 A. Wingert, M. D. Lichter and S. Dubowsky, *IEEE/ASME Trans. Mechatron.*, 2006, **11**, 448.
19 J. W. Fox and N. C. Goulbourne, *J. Mech. Phys. Solids*, 2008, **56**, 2669.
20 I. Müller and P. Strehlow, *Rubber and Rubber Balloons: Paradigms of Thermodynamics*, Springer-Verlag, Berlin Heidelberg, 2004.
21 A. N. Gent, *Rubber Chem. Technol.*, 1996, **69**, 59.
22 E. Mockensturm and N. Goulbourne, *Int. J. Nonlinear Mech.*, 2006, **41**, 388.
23 J. Zhu, S. Cai and Z. Suo, *Int. J. Solids Struct.*, 2010, **47**, 3254.
24 G. Kofod, P. Sommer-Larsen, R. Kornbluh and R. Pelrine, *J. Intell. Mater. Syst. Struct.*, 2003, **14**, 787.
25 S. J. A. Koh, *et al.*, *IEEE/ASME Trans. Mechatron.*, 2011, **16**, 33.
26 S. Rosset, M. Niklaus, P. Dubois and H. R. Shea, *J. Microelectromech. Syst.*, 2009, **18**, 1300.
27 Z. B. Yu, *et al.*, *Appl. Phys. Lett.*, 2009, **95**, 192904.
28 F. Carpi, G. Frediani, M. Nanni and D. De Rossi, *IEEE/ASME Trans. Mechatron.*, 2011, **16**, 16.

